THE SPECTRUM OF QUANTUM CHROMODYNAMICS: A NEW APPROACH TO LATTICE COMPUTATION OF QUARK PROPAGATORS*

By J. Wosiek

Institute of Computer Science, Jagellonian University, Cracow**

(Received June 20, 1986)

A new method of computing quark propagators on a lattice is developed. It reduces the four-dimensional problem to the series of inversions of the two-dimensional fermionic matrices. The technique is applied to compute chiral properties of quantum chromodynamics, and to obtain masses of the lowest lying hadrons.

PACS numbers: 12.38.Gc

1. Introduction

For some time quantum chromodynamics has gained a status of the theory of strong interactions. The spectacular success in describing the short distance phenomena triggered many attempts to obtain predictions of the theory also in its nonperturbative — large distance, domain. At present, the only way to achieve this goal is through the lattice formulation of QCD. Its strong coupling expansion reveals the confinement of quarks and formation of flux tubes. On the weak coupling side, we recover the perturbative expansion of the continuum theory. In addition, one predicts a universal and well defined scaling which must hold while approaching the continuum limit. Nonperturbative predictions are obtained with the aid of the Monte Carlo calculations. To this end one uses techniques well known from statistical physics. However, introduction of the fermionic degrees of freedom requires the development of new methods. Therefore, in spite of the fact that many physical results are already available, the search for new algorithms is by no means a closed subject.

We have developed a new method for computing a quark propagator in an external field, and applied it to the lattice QCD. Propagator of a quark is the basic block in constructing hadronic propagators, and hence, in calculating the spectrum of elementary particles. For this reason, an effective technique for computing propagation of elementary matter field is needed in every lattice simulations of QCD with fermions.

* This work was partly supported by the Polish Atomic Agency, Grant no. CPBP 01.03.

** Address: Instytut Informatyki UJ, Reymonta 4, 30-059 Kraków, Poland.

Plan of this paper is the following. In Chapter 2 we introduce basic concepts of lattice gauge theories, and discuss shortly their various applications. Chapter 3 contains the construction of fermions on a lattice which will be needed for latter study. Our method of computing quark propagators is presented in Chapter 4. Application to QCD without dynamical quarks and our results on hadronic spectrum are discussed in Chapter 5. Summary and conclusions fill Chapter 6.

2. *General formalism and survey of the subject*

Consider four-dimensional, hypercubic lattice of the size $T \times L^3$. To every oriented link l, labelled by (n, μ), assign a SU(3) matrix $U_\mu(n)$. The action of the pure gauge field reads [1]

$$S_G = \beta \sum \mathrm{Tr}\,(U_\square + U_\square^+), \tag{2.1}$$

where $U_\square$ is the product of the link variables along the elementary oriented plaquette, and the sum runs over all plaquettes on the lattice; $\beta = 6/g^2$, g being the bare coupling constant.

Statistical system defined by (2.1) is intensively studied and the structure of the underlying continuum theory slowly emerges [2]. Central question: how close can we approach the continuum limit, with the available resources, is being asked from various perspectives. Measurements of the string tension have confirmed the confinement of colour charges — a unique property of nonabelian gauge theories. It has been expected for a long time, but proved only in the strong coupling regime on a lattice. An approximate scaling was shown to hold for $\beta \geqslant 6.0$, indicating that we may approach the continuum physics [3]. Masses of glueballs were also measured, and data are consistent with scaling [4]. Another result of physical interest concerns the existence of the deconfining phase transition to the gluon plasma [5]. Study of this phenomenon, which occurs at finite temperature, is also done with the action (2.1). In this approach, the size of the lattice, say in T direction, controls the physical temperature of the gluonic system. The transition temperature T_c was found to scale for $6.0 < \beta < 6.3$, demonstrating again the onset of the continuum behaviour. Finally, the original program of Wilson [6] is vigorously continued, and provides direct information about the renormalization group flow of the gauge coupling constants [7].

Construction of the complete quantum chromodynamics on a lattice is achieved by adding to (2.1) the contribution from matter fields [1]

$$S_F = -a^3 \sum_n \{K \sum_\mu [\bar\psi(n)\,(r-\gamma_\mu)U_\mu(n)\psi(n+\mu) + \bar\psi(n+\mu)\,(r+\gamma_\mu)U_\mu^+(n)\psi(n)]$$

$$-\bar\psi(n)\psi(n)\} \equiv \sum_{n,m} \bar\psi(n) M_F(n, m)\psi(m). \tag{2.2}$$

Here, the Dirac fields $\psi(n)$ are assigned to each lattice site. They are in the fundamental representation of the $SU(3)_{colour}$ and also carry a flavour index which will be suppressed in the following. Parameter r distinguishes various formulations and will be discussed in

the next Chapter. Due to the Pauli principle, quark fields in the Lagrange formulation are described by the classical Grassmann variables [8]. The Euclidean path integral for the full theory reads:

$$Z = \int [dU d\psi d\bar{\psi}] e^{-(S_G + S_F)}, \tag{2.3}$$

where Haar integrations are performed over all link SU(3) matrices and Grassmann integrals over $\psi(n)$ and $\bar{\psi}(n)$ variables.

Common approach to (2.3) is to integrate out the quark fields explicitly, since the integrand is Gaussian in ψ,

$$Z = \int [dU] \det (M_F[U]) e^{-S_G[U]}, \tag{2.4}$$

and to treat the remaining integration by Monte Carlo. Direct stochastic evaluation of (2.3) is practically impossible due to the non-positivity of the Grassmann integrations. On the other hand, the statistical system with the partition function (2.4) is well defined (det $M[U]$ is positive definite) but the new effective action is nonlocal. Therefore, Monte Carlo simulations of the full QCD with dynamical fermions use a lot of CPU time, and only very recently some results on moderate size lattices (10^4) became available [9].

Computation of hadronic spectrum, considered by many as an ultimate test of the theory, has only begun [10]. With dynamical quarks, however, extraction of masses of various resonances is obscured by the continuous background of lower mass pairs. This is particularly annoying in the Euclidean formulation of the theory. New methods must be developed to analyse the "data" from the MC simulations with quark loops. Nevertheless, some results obtained with dynamical quarks (contained in det M) are rather encouraging. Studying the $q\bar{q}$ potential in the full SU(2) theory, Schmidt [11] has found indications of the Debye screening. Also an effect of the virtual $q\bar{q}$ pairs on the transition temperature to the quark-gluon plasma was found consistent with the intuitive expectations [12].

As was mentioned above, the effective Boltzmann factor in (2.4) is a nonlocal function of the gauge configuration $\{U\}$. This means that all the simplicity (and speed) of the local thermalization algorithm (e.g. Metropolis or heat bath) is lost and replaced by the tedious evaluation of the determinant of the huge matrix, for each update (change) of *every* link variable. Still, the two existing techniques which deal with the problem, succeed quite remarkably in reducing a number of operations necessary to include the determinant [13, 14]. Nevertheless, the CPU time required for simulations with dynamical fermions is about three orders of magnitude bigger than the one needed if the quark loops are neglected [20]. In view of this situation a recent proposal to apply a complex Langevin technique *directly* to the partition function (2.3) or to its Hamiltonian version is very interesting [15], though at present this approach is applicable only to the two-dimensional models [16]. Together with the proposed in Ref. [17] local representation of fermions in 3+1 dimensions, it may form a useful approach to the notoriously difficult problem of dynamical quarks.

A lot of information about the spectrum of hadrons was obtained in the so-called quenched approximation proposed first by Weingarten [18] and by Parisi and Hamber [19].

In this approach one neglects influence of fermions on the gauge field. Quarks are viewed as propagating in the fluctuating background of the quantum Yang-Mills field. Any feedback from fermionic degrees of freedom is ignored. Hence the name of this scheme, borrowed from the theory of alloys in metallurgy. Technically, the quenched approximation amounts to setting $\det M = 1$, since the determinant describes the net effect of the fermionic field. The remaining influence of quarks shows up only in the various observables which can be built from the ψ variables. Consider, as an example, $\langle \bar{\psi}\psi \rangle$ — the average value of the quark condensate:

$$\langle \bar{\psi}(n)\psi(n) \rangle = \frac{1}{Z} \int [dU d\psi d\bar{\psi}] \bar{\psi}(n)\psi(n) e^{-(S_G + S_F)}. \tag{2.5}$$

Integration over Grassmann variables yields

$$\langle \bar{\psi}(n)\psi(n) \rangle = \frac{1}{Z} \int [dU] \, (M_F^{-1}[U])_{nn} \det (M_F[U]) e^{-S_G}, \tag{2.6}$$

i.e., one must average the inverse of the fermionic matrix (2.2) over the quantum fluctuations of the gauge field. In the quenched approximation, the link variables have an unmodified $\exp(-S_G)$ distribution of the pure Yang-Mills theory.

For mass calculations one uses more complicated observables on the RHS of Eq. (2.6). In general they are fourth (sixth) order polynomials in the fermion field. Using known symmetries of the theory suitable combinations of the ψ and $\bar{\psi}$ are built in order to select separate propagation channels (see next Chapter). Correspondingly, one averages some combinations of the inverse fermionic matrix

$$(M_F^{-1}[U])_{nm} = S(n, m, [U]) = \langle \psi(n)\bar{\psi}(m) \rangle_{\psi\bar{\psi}}, \tag{2.7}$$

which is nothing but the gauge covariant propagator of a quark in a background gluonic field.

The problem of nonlocality in generation of the gauge configurations has been avoided in a quenched approximation. However, fermionic observables are nonlocal functionals of the gauge field U. Therefore, computation of the spectrum of hadrons calls for a lot of computer time even in the quenched approximation. For this reason a search for effective algorithms for computing quark propagators still continues [20, 21, 42]. Of course, the study of fast methods of inversion of large sparse matrices is also relevant for the unquenched theory. In the latter, the inverse matrix is also needed for updating the determinant in addition to constructing fermionic operators.

Finally, we would like to discuss the extraction of the mass parameters from the Monte Carlo "experiments". Detailed formulas depend on the discretization chosen for fermions and will be derived in the next Chapter. Here, we present only the general approach. Consider the evaluation of the partition function (2.3) in the temporal gauge $U_0(n) = 1$. Then, all the integration variables can be divided into T groups $\{U_k(i, n), \psi(i, n), \bar{\psi}(i, n)\} = S_i$, $i = 1, \ldots, T$, each group belonging to one three-dimensional time

slice $n_t = i$. Then Z can be written in the form

$$Z = \sum_{s_1,s_2,\ldots,s_T} \mathscr{T}_{s_1 s_2} \mathscr{T}_{s_2 s_3} \ldots \mathscr{T}_{s_T s_1} = \mathrm{Tr}\, \mathscr{T}^T, \tag{2.8}$$

$\mathscr{T}$ is the transfer matrix of lattice theory [22], and the lattice Hamiltonian is defined by $\mathscr{T} = \exp(-aH)$, a being the lattice spacing. For large T,$Z \sim \lambda_0^T$, where λ_0 is the maximum eigenvalue of the transfer matrix[1]. Equation (2.8) is nothing but the lattice version of the Feynman-Kac formula [23]. Consider now the general Green function

$$\langle O(t_1)O(t_2)\rangle = \frac{1}{Z}\int [dU d\psi d\bar{\psi}] O(t_1)O(t_2)e^{-S} \tag{2.9}$$

for arbitrary integer times $t_1 < t_2$, $t = t_2 - t_1$. It is readily seen that

$$\begin{aligned}\langle O(t_1)O(t_2)\rangle &= \mathrm{Tr}\,(O\mathscr{T}^t O\mathscr{T}^{T-t})/\mathrm{Tr}\,\mathscr{T}^T \\ &\cong \lambda_0^{-T}\sum_{k,l}\lambda_k^t\lambda_l^{T-t}|\langle k|O|l\rangle|^2 \\ &\cong R_1[(\lambda_1/\lambda_0)^t + (\lambda_1/\lambda_0)^{T-t}],\end{aligned} \tag{2.10}$$

where only leading contributions, for large t and $T-t$, have been retained. In terms of the energies

$$\langle O(t_1)O(t_2)\rangle = R_1[e^{-(E_1-E_0)at} + e^{-(E_1-E_0)(T-t)a}] + \ldots, \tag{2.11}$$

where dots denote contributions from the higher excitations. What particular state dominates the sum (2.11), depends on the matrix element $\langle 0|O|k\rangle$. In principle, constructing appropriate operator O, one could excite only single state from the vacuum. In practice we use lattice symmetries in order to restrict maximally the number of states contributing to (2.11). This will be discussed in the next Chapter.

3. Fermions on a lattice

3.1. Species doubling and Wilson formulation

The simplest lattice action for free fermions reads:

$$S_N = \frac{a^3}{2}\sum_{n,\mu}[\bar{\psi}(n)\gamma_\mu\psi(n+\mu) - \bar{\psi}(n+\mu)\gamma_\mu\psi(n)] + ma^4\sum_n \bar{\psi}(n)\psi(n), \tag{3.1}$$

and corresponds to $r = 0$ in the expression (2.2). Classical continuum limit of Eq. (3.1) gives obviously the Dirac action. Note that the first derivative is approximated by the difference of the fermion field taken over *two* lattice spacings. Only such a choice results

[1] Incidentally an Euclean Monte Carlo appears to be the most effective method to diagonalize $\mathscr{T}$, hence also the Hamiltonian.

in the hermitian action, which in turn is necessary for positive definite transfer matrix [22]. This is different from the bosonic case, where the *second* derivative is defined over two lattice spacings.

From (3.1) one obtains the propagator

$$S(k) = [i \sum_{\mu} \gamma_{\mu} \sin(ak_{\mu}) + ma]^{-1}, \qquad -\pi < ak_{\mu} < \pi, \tag{3.2}$$

which reduces to the standard form when $ka \to 0$. However, some other excitations also survive in the continuum limit $a \to 0$. They correspond to the corners of the Brillouin zone $ak_{\mu} = \pm\pi + aq_{\mu}$, for such momenta propagator reduces again to the familiar continuum form exhibiting a free particle pole at $q^2 \sim 0$. This is the famous species multiplication discussed extensively by many authors [24–26]. In particular, existence of species doubling was proved by Nielsen and Ninomya under rather general assumptions of hermiticity, locality and translational invariance [24]. We would like to emphasize here the difference between the fermionic and bosonic cases. Nilsen and Ninomya showed that in general $\sin(k_{\mu}a)$ in (3.2) is replaced by a function $F(k_{\mu}a)$ which has a single zero at $k_{\mu}a = 0$, and is periodic. Therefore $F(k_{\mu}a)$ must have at least a second zero in the Brillouin zone. For bosons, however, F has a *double* zero at the origin, hence no species doubling is implied. The last property can be traced back to the different discretization of the kinetic term in the action, as discussed above. To conclude, the multiplication of fermionic modes occurs because only shifts by *even* number of links represent the space translations. Single link shifts mix various "internal" modes even in the naive formulation.

Two approaches are commonly used to cope with additional states. In the original Wilson formulation one uses the action (Eq. (2.2) with $r = 1$, and $U = 1$)

$$S_{\mathrm{W}} = \sum_{n} \{\bar{\psi}(n)\psi(n) - K \sum_{\mu} [\bar{\psi}(n)(1-\gamma_{\mu})\psi(n+\mu) + \bar{\psi}(n+\mu)(1+\gamma_{\mu})\psi(n)]\}. \tag{3.3}$$

It has the appropriate continuum limit if $K = (8+2ma)^{-1}$. All additional excitations acquire a mass $M \sim 1/a$ and decouple in the continuum limit. However, chiral symmetry is now explicitly broken even if $m = 0$ ($K = 1/8$). Nonsymmetric terms vanish only when $a \to 0$. Therefore, chiral symmetry of the continuum theory together with its spontaneous breakdown are expected to be recovered only in the limiting transition.

Lack of the chiral symmetry introduces additional difficulty in extracting physical quantities from lattice simulations. The hopping parameter K (or equivalently the bare mass of a quark m) is renormalized by quantum fluctuations. On the other hand, K is the direct input parameter controlling all physical observables. Commonly adopted procedure consists in computing measurable quantities for a series of K values, and then extrapolating them towards an unknown, a priori, point $K = K_{\mathrm{c}}$. K_{c} corresponds to the chirally symmetric quantum theory, and is determined by vanishing of the pion mass. This procedure introduces additional uncertainty since K_{c} fluctuates with gauge configurations. Also extraction of the renormalized current mass of a quark becomes tricky. Finally, numerical computations of quark propagators require four times more memory and CPU time than the staggered fermion approach (see below).

However, quantum number content of various operators is very transparent in Wilson approach. Also introduction of the explicit flavour breaking is simple. For this reason Wilson fermions are intensively used by groups with large computing resources [27–30].

3.2. Kogut-Susskind fermions

In this formulation, often referred to as staggered fermions [31–34], one saves a lot of the computer storage paying the price of rather messy quantum number analysis. Since we shall be using this approach later on, it will be discussed now in some details.

It turns out that one can pre-diagonalize the action (3.1) [35]. Define a new four-component field $\chi^b(n)$, $b = 1, \ldots, 4$,

$$\psi(n) = A(n)\chi(n), \qquad \bar{\psi}(n) = \bar{\chi}(n)A^\dagger(n), \tag{3.4}$$

with

$$A(n) = \gamma_1^{n_1}\gamma_2^{n_2}\gamma_3^{n_3}\gamma_4^{n_4}, \qquad n = (n_1, n_2, n_3, n_4). \tag{3.5}$$

Since

$$A^\dagger(n)\gamma^\mu A(n+\mu) = (-1)^{n_1+\cdots+n_{\mu-1}} \equiv \alpha_\mu(n)\mathbf{1}, \tag{3.6}$$

all four components χ^b decouple

$$S_F = \sum_{b,n}\left\{\frac{a^3}{2}\sum_\mu \alpha_\mu(n)\left[\bar{\chi}^b(n)\chi^b(n+\mu) - \bar{\chi}^b(n+\mu)\chi^b(n)\right] + ma^4\bar{\chi}^b(n)\chi^b(n)\right\}. \tag{3.7}$$

The same trick works for the full interacting theory: all 64 modes are grouped into four identical groups, each group containing 16 interacting excitations. From now on, we will skip the index b on the χ field and restrict the analysis to one copy. Remaining degrees of freedom will be soon interpreted as four flavours of a Dirac fermion. Before doing so, let us discuss the chiral properties of the theory.

It is readily seen from (3.7) that kinetic term couples χ on even (odd) sites with $\bar{\chi}$ on odd (even) sites only. Therefore the theory has a global $U(1)\times U(1)$ symmetry:

$$\chi(\text{even}) \to e^{i\alpha}\chi(\text{even}), \qquad \bar{\chi}(\text{odd}) \to \bar{\chi}(\text{odd})e^{-i\alpha},$$

$$\chi(\text{odd}) \to e^{i\beta}\chi(\text{odd}), \qquad \bar{\chi}(\text{even}) \to \bar{\chi}(\text{even})e^{-i\beta}, \tag{3.8}$$

for $m = 0$. This is all what remains from the full chiral SU(f)×SU(f) invariance of the continuum action. However, this remnant of chiral symmetry is sufficient to protect quark mass against renormalization when $m = 0$. Contrary to the Wilson case, we know a priori that the chiral limit of the renormalized theory remains at $m = 0$. Therefore, we know where to extrapolate physical observables measured for various m's.

In addition, one can study spontaneous breaking of the lattice chiral symmetry as anticipated from the continuum physics. It should be stressed, however, that this study provides only some clues about the analogous phenomenon in the continuum. The real

question is: do we see signs of the restoration of the full chiral group? In other words, do other members of the pseudoscalar octet become light, ultimately degenerate, with the single Goldstone boson expected from (3.8)? A substantial amount of the human and computer effort is being spent to answer these questions [37, 39].

Spin diagonalization (3.6) works without any change also for the interacting theory. The coupled action reads:

$$S_{\mathrm{KS}} = a^3 \sum_n \{\tfrac{1}{2} \sum_\mu [\bar\chi(n)\alpha_\mu(n) U_\mu(n)\chi(n+\mu) - \bar\chi(n+\mu)\alpha_\mu(n) U_\mu^\dagger(n)\chi(n)] + ma\bar\chi(n)\chi(n)\}. \quad (3.9)$$

Spin and flavour structure can now be rediscovered by regrouping all 16 modes of the χ field [25, 32]. Consider splitting of the whole lattice into elementary hypercubes labelled by even sites

$$n_\mu = 2N_\mu + \eta_\mu, \qquad \eta_\mu = 0,1; \qquad \mu = 1, \ldots, 4. \quad (3.10)$$

Sixteen four-vectors η point towards the corners of a hypercube. Define a new 16-component field on a blocked lattice

$$\chi_\eta(N) = (-1)^N \chi(2N+\eta), \qquad \bar\chi_\eta(N) = (-1)^N \bar\chi(2N+\eta),$$
$$(-1)^N = (-1)^{N_1+N_2+N_3+N_4}. \quad (3.11)$$

The 16-component quark field on the coarser lattice is a linear combination of χ_η

$$q^{\alpha a}(N) = \tfrac{1}{8} \sum_\eta \Gamma_\eta^{\alpha a} \chi_\eta(N), \qquad \bar q^{\alpha a}(N) = \tfrac{1}{8} \sum_\eta \Gamma_\eta^{*\alpha a} \bar\chi_\eta(N), \quad (3.12)$$

where

$$\Gamma_\eta = \gamma_1^{\eta_1} \gamma_2^{\eta_2} \gamma_3^{\eta_3} \gamma_4^{\eta_4}. \quad (3.13)$$

The Greek and Latin indices label the Dirac and flavour degrees of freedom. Inverse transformation reads:

$$\chi_\eta(N) = 2 \sum_{\alpha,a} \Gamma_\eta^{*\alpha a} q^{\alpha a}(N), \qquad \bar\chi_\eta(N) = 2 \sum_{\alpha,a} \bar q^{\alpha a}(N) \Gamma_\eta^{\alpha a}. \quad (3.14)$$

Structure of Eqs (3.12) and (3.14) suggests treating internal 16 dimensional space as the tensor product of the Dirac and flavour spaces. Indeed, in terms of the quark field the action takes the form

$$S_{\mathrm{KS}} = (2a)^4 \sum_N \{\sum_\mu \bar q(N) [(\gamma_\mu \otimes \mathbf{1}) \Delta_\mu + a\gamma_5^\dagger \otimes t_5^\dagger \delta_\mu] q(N) + m\bar q(N) q(N)\}, \quad (3.15)$$

where

$$\Delta_\mu q(N) = \frac{1}{4a} [q(N+\mu) - q(N-\mu)],$$

$$\delta_\mu q(N) = \frac{1}{4a^2} [q(N+\mu) - 2q(N) + q(N-\mu)],$$

and matrices γ_μ and t_μ act on the spin and flavour indices, respectively. Convenient representation of t_μ is $t_\mu = \gamma_\mu^*$.

From the Fourier transform of (3.15) one gets the free propagator

$$\Delta(k) = \frac{2}{(ma)^2 + \sum_\mu \sin^2(ak_\mu)} \left\{ \sum_\mu \left[i \sin(ak_\mu)(\gamma_\mu \otimes \mathbf{1}) \right.\right.$$

$$\left.\left. -(\cos(2ak_\mu) - 1)(\gamma_5^\dagger \otimes t_\mu^\dagger t_5) \right] - 2ma(\mathbf{1} \otimes \mathbf{1}) \right\} \tag{3.16}$$

which has only one pole in the Brillouin zone $-\frac{\pi}{2} < ak_\mu < \frac{\pi}{2}$, as desired. In the continuum limit the first and third terms reproduce the standard Dirac propagator, second term being higher order in a. On the lattice, however, this term is a source of some artefacts. It generates flavour changing interactions which remain also in the coupled theory. Secondly, it breaks parity, and hence one is not able to separate directly opposite parity states in this approach.

The simple strategy to identify particular channels is the following (see the next Section). One builds corresponding correlation functions in the q representation using symmetries of the continuum theory. Then, everything is transformed into the χ representation which is much easier to handle numerically. Another approach analyses the χ formulation with respect to the full discrete symmetry group of the lattice action (3.9) [36, 38, 39]. In particular, the field combinations belonging to the irreducible representations of this group were found, and their composition in terms of the continuum symmetry identified.

3.3. Hadronic operators

Before we review the construction of hadronic operators for staggered fermions, let us elucidate an effect of additional modes on the example of the naive approach (3.1).

A. Quantum numbers in the naive case

It is enough to consider a free case since interactions do not change the quantum number content of various operators. The lattice propagator (3.2) of a free fermion reads:

$$S(n, 0) \equiv S(n) = \int \frac{d^4\kappa}{(2\pi)^4} e^{in\kappa} \frac{ma - i\gamma_\mu s_\mu(\kappa)}{(ma)^2 + s^2(\kappa)}, \tag{3.17}$$

where $-\pi < \kappa_\mu < \pi$, and $s_\mu = \sin(\kappa_\mu)$. In the continuum limit (3.17) acquires contributions from the 3^4 regions of the Brillouin zone (see Fig. 1 for a two-dimensional example):

$$\kappa_\mu = \varepsilon_\mu^{(i)}\pi + ap_\mu, \qquad \varepsilon_\mu^{(i)} = 0, \pm 1; \qquad i = 1, \ldots, 3^4.$$

Expanding (3.17) and merging together contributions from $\varepsilon_\mu^{(i)} = \pm 1$, gives

$$\lim_{a \to 0} a^{-3} S(n) = \sum_\eta (-1)^{n \cdot \eta} S_F(x_\eta), \tag{3.18}$$

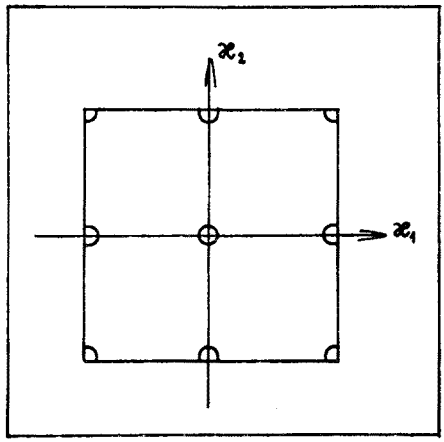

Fig. 1. Location of the fermionic modes which are important in the continuum limit of the two-dimensional propagator (cf. Eq. (3.17))

where we have defined

$$x_\eta^\mu = \begin{cases} an^\mu, \eta^\mu = 0, \\ -an^\mu, \eta^\mu = 1, \end{cases} \quad \eta^\mu = 0,1$$

and $S_F(x)$ is the continuum Feynman propagator:

$$S_F(x) = \int \frac{d^4p}{(2\pi)^4} e^{ipx} \frac{m + i\not{p}}{m^2 + p^2} . \tag{3.19}$$

Equation (3.18) gives directly contributions of additional species to the quark propagator. Important point for the sequel is that $S_F(an)$ is a *smooth* function of n, while the lattice propagator $S(n)$ is not. Characteristic phase factors $(-1)^n$ have been factored out explicitly in (3.18) and will be used later on to identify various modes.

Consider now, as an example, a correlation function in the naive pseudoscalar channel. The Grassmann integrations give

$$\langle \bar{\psi}(n)\gamma^5\psi(n)\bar{\psi}(0)\gamma^5\psi(0)\rangle = \mathrm{Tr}\,[\gamma^5 S(n,0)\gamma^5 S(0,n)] \equiv K(n). \tag{3.20}$$

Zero momentum channel is projected out by summing Eq. (3.20) over $\vec{n}$

$$M_{PS}(n_t) = \sum_{\vec{n}} \mathrm{Tr}\,[\gamma^5 S(n)\gamma^5 S(-n)]. \tag{3.21}$$

We substitute (3.18) into (3.21) and look for the contributions which are important in the continuum limit. Clearly, M_{PS} has a structure:

$$M_{PS}(n_t) = A_{PS}(n_t) + B_{PS}(n_t) \cdot (-1)^{n_t}. \tag{3.22}$$

It is crucial to realize that only certain pairs of modes survive summation over n in the $a \to 0$ limit. Due to the smoothness of $S_F(an)$, only diagonal terms would be free from

the oscillating factors $(-1)^n$ and would not vanish when $a \to 0$. In the case of the amplitude B, products differing only by the $(-1)^{n_t}$ would contribute. Next, we observe that

$$S_F(x_\eta) = \Gamma_\eta S_F(x)\Gamma_\eta^\dagger, \quad \eta^2 \text{ even},$$
$$\gamma^5 S_F(x_\eta)\gamma^5 = \Gamma_\eta S_F(x)\Gamma_\eta^\dagger, \quad \eta^2 \text{ odd}, \tag{3.23}$$

with x_η and Γ_η defined in (3.18) and (3.13), respectively. Using this relation to eliminate partly reflected arguments in S_F, we obtain finally

$$M_{PS}(n_t) = M_{\gamma^5}(n_t) + (-1)^{n_t} M_{\gamma^4}(n_t), \tag{3.24}$$

where

$$M_\Gamma(n_t) = \sum_{\vec{n}} \mathrm{Tr}\,[\Gamma S_F(an)\Gamma S_F(-an)] \tag{3.25}$$

have well defined quantum numbers in the center of mass frame. We see that a pseudoscalar and scalar states couple to the naively defined pseudoscalar channel.

Other channels are separated if we insist on different pairing of modes in (3.21). This is achieved by summing over $\vec{n}$ with suitable phase factors. If we define

$$M_{VT}(n_t) = \sum_{\vec{n}} [(-1)^{n_x} + (-1)^{n_y} + (-1)^{n_z}]K(n),$$
$$M_{PV}(n_t) = \sum_{\vec{n}} [(-1)^{n_x+n_y} + (-1)^{n_x+n_z} + (-1)^{n_y+n_z}]K(n),$$
$$M_S(n_t) = \sum_{\vec{n}} (-1)^{n_x+n_y+n_z} K(n), \tag{3.26}$$

then one finds contributions listed in Table I (see Appendix for more detailed derivation). This concludes the quantum number analysis of the naive approach. Since the naive and staggered formulations are basically related by the unitary transformation (3.4), results in the staggered formulation are the same [37] but require longer derivation. In exchange for this effort one is able to discuss partly the flavour content of the theory.

TABLE I

Quantum number content of mesonic channels in the naive and staggered fermion formulations[1]

Amplitude	Phase factor	Operator		J^{PC}		State	
		A	B	A	B	A	B
PS	1	γ^5	γ^4	0^{-+}	0^{+-}	π	
VT	$(-1)^{n_x}+(-1)^{n_y}+(-1)^{n_z}$	γ^i	$\gamma^j\gamma^k$	1^{--}	1^{+-}	ϱ	B
PV	$(-1)^{n_x+n_y}+(-1)^{n_x+n_z}+(-1)^{n_y+n_z}$	$\gamma^i\gamma^4$	$\gamma^j\gamma^k\gamma^4$	1^{--}	1^{++}	$\tilde{\varrho}$	A_1
S	$(-1)^{n_x+n_y+n_z}$	$\gamma^5\gamma^4$	1	0^{-+}	0^{++}	$\tilde{\pi}$	S

[1] The $\tilde{\pi}$ and $\tilde{\varrho}$ states have different flavour content from those coupling to the pseudoscalar and vector channels.

B, Staggered mesons

In the q-representation, the Dirac structure of required operators is obvious. Consider the following currents [32, 37]

$$J_{AB}(N) = \bar{q}(N)\Gamma_A \otimes T_B q(N), \tag{3.27}$$

with Γ_A given in Table I. In principle, the flavour content (T_B) can be chosen independently. In general case, however, resulting currents are nonlocal in the χ representation. Therefore, numerical study of these channels is subject to larger statistical errors — hence, more time consuming. General currents (3.27) have been used to study e.g., restoration of the full SU(f) × SU(f) chiral symmetry [37, 30]. In the following, we will restrict the analysis to hadronic states which saturate the Green functions of the local (in χ representation) currents. This requires $T_B = \Gamma_A^*$.

According to the discussion in Chapter 2 we expect (for small Ma)

$$M_A(N_t) = \sum_{\vec{N}} \langle J_A(N) J_A(0)\rangle$$

$$= K_{P(A)}[e^{-2aM_{P(A)}N_t} + e^{-aM_{P(A)}(T-2N_t)}] + \ldots, \tag{3.28}$$

where dots denote contribution from higher recurrences. On the other hand, correlations of the χ fields are easier to compute numerically; therefore, they are more widely used. With the aid of transformations (3.12) and (3.14) one can relate $M_A(N_t)$ to the four basic Green functions measured in the Monte Carlo experiment [32, 37, 64]. They are given by Eqs (3.21) and (3.26) with $K(n)$ simply related to the propagator of a χ field:

$$K(n) = 4 \sum_{a,b=1}^{3} |\langle \chi^a(n)\bar{\chi}^b(0)\rangle_\chi|^2. \tag{3.29}$$

Note that the correlations (3.26) are defined for all lattice times, while those in Eq. (3.28) are given only for even time separations. Total amount of information contained in both sets of propagators is the same, since we have twice as many functions (3.28), while the correlations (3.28) receive contributions from two channels each. Assuming (3.28), relations between the Green functions (3.28) and (3.26) can be inverted, giving finally

$$\begin{aligned} M_{PS}(n_t) &= E_\pi(n_t), \\ M_{VT}(n_t) &= E_\varrho(n_t) + E_B(n_t)(-1)^{n_t}, \\ M_{PV}(n_t) &= E_{\tilde{\varrho}}(n_t) + E_{A_1}(n_t)(-1)^{n_t}, \\ M_S(n_t) &= E_{\tilde{\pi}}(n_t) + E_S(n_t)(-1)^{n_t}, \end{aligned} \tag{3.30}$$

where

$$E_p(n_t) = R_p[e^{-aM_p n_t} + e^{-aM_p(T-n_t)}] + \ldots,$$

in close agreement with the naive analysis (Table I). Formulas (3.30) are widely used in the literature in order to parametrize MC data and to extract masses of lightest hadrons

[37, 62–66]. Equations (3.30) differ from the expressions derived in Ref. [64] by terms vanishing in the $a \to 0$ limit. However, corrections derived in [64] do not exhaust all the terms of the order $O(a^2)$. For example, the $O(a^2)$ opposite parity contributions to (3.28) were not included. Continuum parity is not conserved on the lattice (γ^5 term in (3.15)). Therefore we expect an $O(a^2)$ contribution from the opposite parity states to (3.28). Also, the group theoretical analysis of Ref. [36] does not confirm any extra terms in (3.30). On the other hand, mixing between the opposite parity states in (3.30) is the genuine property of the staggered formulation reflecting the fact that only even shifts on the K–S lattice represent space translations.

C. Staggered baryons

For baryons, the situation is more complicated [40, 32, 36]. Even in the continuum, baryonic propagators have richer structure than the mesonic ones. Baryons are essentially different from their antiparticles. In particular, the relative parity of a baryon and an antibaryon is -1. Therefore, in a given parity channel, one encounters a baryon and an antiparticle of its opposite parity partner. They can be easily distinguished since they propagate forwards and backwards in time, respectively. As a consequence, baryon propagator is not symmetric on a periodic lattice. For example, in a proton channel $(1/2)^+$ state dominates at small n_t, while a $N(1/2)^-$ resonance determines the slope at small $T-n_t$. In addition, one has mixing of various parity states peculiar to Kogut-Susskind fermions.

The only local baryonic operator reads [32, 36, 40]:

$$\psi^{\alpha a}(N) = \frac{1}{3!}\,\varepsilon_{ijk} \sum_{\eta} \Gamma_\eta^{\alpha\beta}\Gamma_\eta^{*ab} q_i^{\beta b}(N)\,[q_j(N)\,(C\Gamma_\eta \otimes C_\eta^*\Gamma^*)q_k(N)], \tag{3.31}$$

where C is the charge conjugation matrix: $C\gamma_\mu C^\dagger = -\gamma_\mu^*$. In terms of the χ fields, $\psi^{\alpha a}$ is given by

$$\psi^{\alpha a}(N) = \tfrac{1}{8}\sum_\eta \Gamma_\eta^{\alpha a}(-1)^N \psi(2N+\eta),$$

$$\bar\psi^{\alpha a}(N) = \tfrac{1}{8}\sum_\eta \Gamma_\eta^{*\alpha a}(-1)^N \bar\psi(2N+\eta), \tag{3.32}$$

with

$$\psi(n) = \frac{1}{3!}\,\varepsilon_{ijk}\chi_i(n)\chi_j(n)\chi_k(n). \tag{3.32a}$$

Define the field $\psi_\pm^{\alpha a}$ with specific parity

$$\psi_\pm^{\alpha a}(N) = \tfrac{1}{2}(1 \pm \gamma_4)^{\alpha\alpha'}\psi^{\alpha' a}(N). \tag{3.33}$$

Correlation functions in a given parity channel

$$B_\pm(N_t) = \sum_{\vec N,\alpha,a} \langle \bar\psi_\pm^{\alpha a}(N)\psi_\pm^{\alpha a}(0)\rangle \tag{3.34}$$

are expected to have simple behaviour when $a \to 0$. According to the earlier discussion we parametrize B as

$$B_{\pm}(N_t) = K_{\pm} e^{-2aM_{\pm}N_t} + K_{\mp} e^{-M_{\mp} a(T-2N_t)} + \ldots, \tag{3.35}$$

where we have abbreviated $M_{\pm} = M_{N(\frac{1}{2})^{\pm}}$. After some algebra, one obtains

$$B_{\pm}(N_t) = 2B(2N_t) \pm B(2N_t+1) \pm B(2N_t-1). \tag{3.36}$$

$B(n_t)$ is given by

$$B(n_t) = \sum_{\substack{\vec{n} \text{ even} \\ i,j,k,i',k',j'}} \varepsilon_{ijk}\varepsilon_{i'j'k'} \langle \bar{\chi}_i(n)\bar{\chi}_j(n)\bar{\chi}_k(n)\chi_{i'}(0)\chi_{j'}(0)\chi_{k'}(0)\rangle \tag{3.37}$$

and is directly measured in lattice Monte Carlo. Assuming the form (3.35) for $B_{\pm}(N_t)$, one can solve Eq. (3.36) for $B(n_t)$. This gives

$$\begin{aligned} B(n_t) = {} & R_+ \left[e^{-aM_+ n_t} + (-1)^{n_t} e^{-aM_+(T-n_t)} \right] \\ & + R_- \left[(-1)^{n_t} e^{-aM_- n_t} + e^{-aM_-(T-n_t)} \right]. \end{aligned} \tag{3.38}$$

Equations (3.30) and (3.38) will be used in Chapter 4 to extract masses from our Monte Carlo data.

4. The Alternate Direction Implicit method in four dimensions

As was discussed in Chapter 2, computation of hadronic spectrum requires a lot of CPU time even in the quenched approximation. Most of the time is spent on the measurements of hadronic propagators. One constructs the latter from a quark propagator which is nothing but the inverse of a fermionic matrix defining the action of matter fields (cf. (2.2) and (2.7)). Elements of the inverse matrix are nonlocal functionals of a gauge field. Modifications of $M^{-1}[U]$ resulting from a local change of a single link variable cannot be calculated just in a few operations, as is the case for the pure gauge Boltzmann factor. On the other hand, computer effort required for the measurement of $M^{-1}[U]$ is smaller by orders of magnitude from that needed in the unquenched approximation. In the latter case one must know $\det(M)$ (or equivalently M^{-1}) to decide on *every* update of *each* link variable. Therefore, fast algorithms for inversion of the large sparse systems are in demand and study of new methods continues [20, 21, 42]. The most popular is the conjugate gradients technique of Hestens and Stiefel [43].

We will present results of the application of the generalization of the Alternate Directions Implicit (ADI) method to the problem [44, 45, 46]. This algorithm gives, in our opinion, more physical insight into the very process of inversion. At the same time it is particularly suited for vector computers.

The method is the following. Consider the system of linear equations

$$M_F X = B, \tag{4.1}$$

with the right hand side describing a unit source[2]. Assume that the matrix M_F can be decomposed into a sum

$$M_F = \Sigma_1 + \Sigma_2. \tag{4.2}$$

Then, one can rewrite above equations in the form

$$\begin{aligned}(r+\Sigma_1)X &= (r-\Sigma_2)X+B,\\ (r+\Sigma_2)X &= (r-\Sigma_1)X+B,\end{aligned} \tag{4.3}$$

with the auxiliary relaxation parameter r. Define the iterative procedure $X^{(0)} = B$

$$\begin{aligned}X^{(N+1/2)} &= (r+\Sigma_1)^{-1}[(r-\Sigma_2)X^{(N)}+B],\\ X^{(N+1)} &= (r+\Sigma_2)^{-1}[(r-\Sigma_1)X^{(N+1/2)}+B].\end{aligned} \tag{4.4}$$

For suitable r, $X^{(N)}$ converges to the solution $X = M_F^{-1}B$. We work with Kogut-Susskind fermions in four dimensions ($M_F = iM_{KS}$, cf. (3.9)). In this case, the most symmetric and optimal splitting of M_F reads:

$$\begin{aligned}2\Sigma_1 &= ima - S_x - S_y, \quad 2\Sigma_2 = ima - S_z - S_T,\\ (iS_\mu)_{nn'} &= \alpha_\mu(n)\,[U_\mu(n)\delta_{n+\mu,n'} - U_\mu^\dagger(n')\delta_{n-\mu,n'}].\end{aligned} \tag{4.5}$$

Matrices $r \pm \Sigma_i$, $i = 1, 2$, describe two-dimensional propagation of a fermion in a background field. They correspond to the set of decoupled two-dimensional theories. We will refer to this property as "dimensional reduction": full ADI iteration is basically composed of two inversions of the fermionic matrices restricted to the two (alternating in their orientations) planes. These are completely decoupled procedures and can be easily vectorized. Also a simple and rather flexible segmentation of the algorithm is possible. In the most extreme case, only one plane of the link and fermionic variables must reside in the fast memory at each stage of the computations.

The rate of convergence of (4.4) depends on the value of r. We have fixed r by minimizing the spectral radius (i.e. the maximal eigenvalue) of the error propagating matrix

$$E = (r+\Sigma_2)^{-1}(r-\Sigma_1)\,(r+\Sigma_1)^{-1}(r-\Sigma_2) \tag{4.6}$$

for free fermions. In this case, $r \pm \Sigma_1$ and $r \pm \Sigma_2$ commute and the problem reduces to finding the minimum of

$$\max \left|\frac{r-\sigma}{r+\sigma}\right|^2, \tag{4.7}$$

σ being the eigenvalue of Σ_i. One obtains $r_0 = i\sqrt{(ma)^2+\lambda_{max}^2}$ with $\lambda_{max} = 2\sqrt{2}$. It turns out that the optimal value of r for the interacting case is smaller than that by ca 30%.

[2] In a recent paper Parisi and Billoire suggested using more complicated RHS for reduction of the statistical noise [47].

This reduction may come from the decrease of the effective range of the eigenvalues resulting from the disordering effect of the gauge variables.

Other choices of r are of course possible. In particular, Wachspress and Jordan have derived separately an iteration dependent set of relaxation parameters $\{r^{(N)}\}$ which minimize the spectral radius of a product E^M for some fixed number of iterations M. In some cases this procedure speeds up the convergence remarkably. Unfortunately, both theories apply only to the positive definite and commuting matrices and cannot be easily extended to our case. One could invert $M_F^\dagger M_F$ instead of M_F, fulfilling at least one of the requirements. Resulting algorithm, however, does not satisfy dimensional reduction and becomes messy.

The ADI approach is useful only when one can simply invert matrices $r+\Sigma_i$. They describe two-dimensional propagation of a fermion in a given background field $\{U\}$. Hence, there is an exciting possibility that $r+\Sigma_i$ could be inverted analytically. Solution of this problem in the U(1) case, in the continuum is known [48]. Recently Rothe has also found corresponding expression in the nonabelian theory [49]. No exact solution on a lattice is known at the moment, therefore, we recede to the numerical approach. Σ_i+r are sparse matrices corresponding to the nearest neighbours interaction on the two-dimensional torus (periodic boundary conditions are used). For an L^4 lattice Σ_i+r are built from $3L\times 3L$ blocks describing one-dimensional propagation of a coloured quark. In terms of these blocks, Σ_i are modified tri-diagonal matrices — modification coming from periodic boundary conditions. We have adapted the recursive Thomas algorithm for solving tri-diagonal systems, and used it to invert $r+\Sigma_i$ exactly. Of course, other methods could be also applied here. Choice of the particular procedure depends on the available resources. One alternative possibility would be the ADI itself. As was discussed earlier, the optimal relaxation parameter is large and imaginary $\mathrm{Im}\, r_0 \sim 1.7$. Therefore, the effective mass for the internal ADI inversions would be large, and corresponding spectral radius is estimated to be $\varrho_{\mathrm{int}} \sim 0.07$. Hence, very few internal iterations would be needed to secure a sufficient accuracy.

Every attempt of inverting M_F faces a problem of the critical slowing down when the quark mass ma becomes small. The eigenvalues of M_F have the form $\nu_k = ima+\lambda_k$, with λ_k varying over the symmetric interval on the real axis. Therefore, it is the quark mass which screens ν_k from being zero. Consequently the rate of convergence of any inversion procedure is decreasing with ma. Common approach to this difficulty is to compute physical quantities for $ma > 0$, and then to extrapolate them to the interesting region $ma = 0$. For this reason, performance of the method for small ma is the crucial check of every procedure.

Our technique was tested on a small $(4^3\times 8)$ lattice. Fig. 2 shows the error Δ, defined to be

$$\Delta(N) = \|M_F X^{(N)} - B\|/\sqrt{N_F}, \qquad N_F = 3T\times L^3, \tag{4.8}$$

as a function of the number of iterations N. Two observations are evident from this graph: 1) the algorithm converges for small quark masses ($ma \geqslant 0.01$) though the critical slowing down is substantial, and 2) it is more effective to reach small quark mass through a series

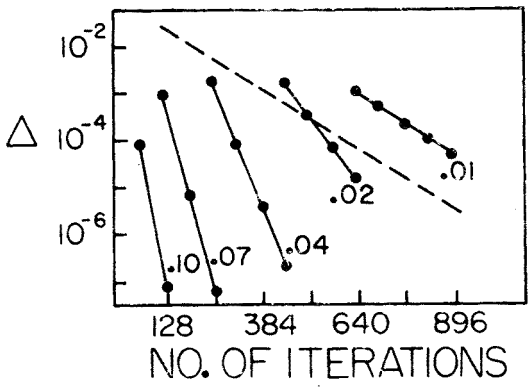

Fig. 2. Dependence of the error of the ADI method (cf. Eq. (4.8)) on the number of iterations, for various values of the quark mass. Dashed line — $ma = 0.01$, $X^{(0)} = B$. Solid line — $X^{(0)}(m_{i+1}) = X^{(N)}(m_i)$

of converging iterations at higher (progressively decreasing) values of ma (solid line), than by performing many iterations starting from $X\langle 0\rangle = B$ at small ma. In the first approach, one generates results for the intermediate masses and prepares better starting point for the next ma.

Further increase of the overall efficiency can be achieved by perturbing $X(m)$ in m while moving to the next value of m. Namely, after converging at given quark mass m_1 to, say, $X(m_1)$, we can use the information contained in all earlier results — $X(m_j)$, $j \leqslant i$ — to extrapolate $X(m_i)$ to m_{i+1}. This procedure improves the starting point for the next mass[3]. With some knowledge of the structure of the singularity at $ma = 0$, one can also use better dependent and independent variables for the extrapolation. With all these tricks we have reached, with the same number of iterations, ten times smaller error at the last value of ma.

We have also looked at the error $\Delta_{\max}$, defined as

$$\Delta_{\max}(N) = \max_i |(M_F X^{(N)} - B)_i|,$$

and for the relative errors corresponding to Δ and $\Delta_{\max}$. Comparison of Δ and $\Delta_{\max}$ tells us how uniform in space is the inversion. Typically, Δ and $\Delta_{\max}$ differed by one order of magnitude. All four errors were falling exponentially with the same slopes.

Fig. 3 presents the spectral radius as extracted from our data, and the one given by the formula (4.7), with the optimal value for $r = r_0$. They agree nicely, for a range of quark masses, provided we choose $\lambda_{\max} = 1.7$ rather than the free value 2.8. As expected, the method would diverge for $ma = 0$. For small ma, critical slowing down becomes a problem for ADI and for other approaches. In this situation the pre-conditioning of M_F proposed in Refs [21, 28] is very promising. The idea of Batrouni et al. is rather general and it would be very interesting to couple it with the ADI approach.

In Fig. 4 we show the comparison of the convergence rates between conjugate gradients and ADI. The conjugate gradient data come from the work of the Wuppertal group

[3] This trick was suggested to me by Ph. De Forcrand.

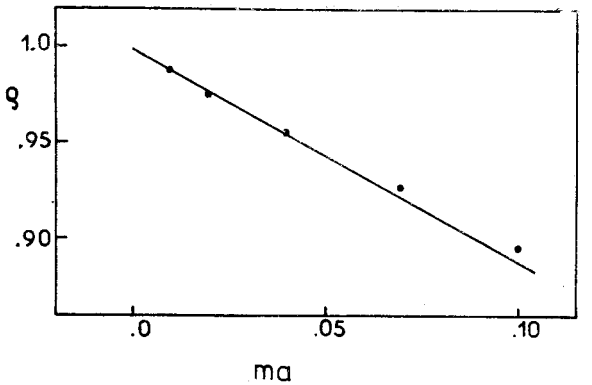

Fig. 3. The spectral radius of the error propagating matrix (4.6). Solid line — exact expression in the free case (cf. Eq. (4.7)). Black points — interacting case, "data" are obtained from the ADI test run

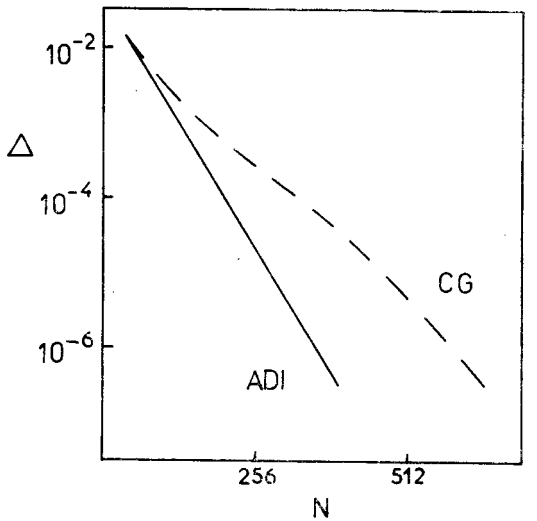

Fig. 4. The error Δ as a function of the number of iterations. Solid line — ADI; dashed line — conjugate gradients (CG)

[29, 52–54]. The CG algorithm converges to the exact answer after at most n iterations, n being size of the matrix. This property is only of the academic interest here, since our problems need $n \sim 10^6$. To reach satisfactory precision ($\Delta \sim 10^{-6}$), ADI required half as many iterations as CG. Similar figure was obtained from the comparison with the data published by Barkai et al. in Ref. [55].

Our algorithm is prepared for effective optimization only on large machines. With ~ 1 MWord of memory[4], much of data independent of the quark propagator, can be precomputed once for all iterations, considerably increasing the speed of the inversion. For

[4] Results presented here were obtained on the CYBER 205 computer in Bochum which has 374 KWords of memory available to the user.

this reason, we have compared here only the rate of convergence of both methods. This parameter is an implementation independent characteristic of a given method. Present version of the ADI program requires $O(\mathcal{N}^{5/4})$ arithmetic operations per iteration. Again, with larger memory available this can be reduced to $O(\mathcal{N})$, $\mathcal{N}$ being the number of lattice sities.

Taking into account other properties (physical appeal of the dimensional reduction, easy vectorization and flexible segmentation), we feel that ADI is a useful alternative to conjugate gradients and other methods of inversion of the large sparse matrices. The following discussion of our results on the quenched QCD demonstrates the capability of this approach.

5. *Results*

We used the ADI method to study the lattice QCD in the quenched approximation. Preliminary results of this calculation were reported elsewhere [45, 46]. The simulation was done on the 16×8^3 lattice at $\beta = 6.0$ using the CYBER 205 computer in Bochum. With Kogut-Susskind fermions we succeeded in packing the whole problem into 375 KWord memory of the Bochum machine, partly at the expense of the speed of the algorithm. The SU(3) algebra was performed using the 8-bit coding technique of Bunk et al. [52]. This is a very effective, space saving method which requires only one CDC word to store an SU(3) matrix. Twelve uncorrelated gauge configurations were used for averaging fermionic observables. The configurations were prepared starting with twelve larger (28×16^3) well thermalized configurations, generated by A. König for other purposes [53]. Smaller configurations were cut out from large lattice and then, imposing periodic boundary conditions on 16×8^3 lattice, we ran 400 sweeps in order to thermalize the local heating at the boundaries. Thermalization was performed with the aid of the RAUPE program written in Wuppertal by Schilling et al. [54].

In principle, ADI works for arbitrary small $ma > 0$. Spectral radius, as given by Eq. (4.7), (with $r = r_0$) is smaller than 1 for $ma > 0$. Aside from the critical slowing down, however, it is not recommended to go to the too small bare mass of a quark on a finite lattice. With decreasing ma, the finite size effects become more pronounced. This bias is strongest in the Goldstone boson channel. Correlation length tends to infinity when $ma \to 0$ and the influence of the boundaries grows accordingly. Therefore we have restricted quark masses to $ma = 0.16$, 0.09, 0.04 and 0.0225. Nevertheless, during the tests, our method performed satisfactorily also for smaller mass (= 0.01, cf. Fig. 1). Barkai, Moriarty and Rebbi have achieved smallest, up to date, value of $ma = 0.01$ on a 32×16^3 lattice [62]. However, recent study of a finite size effects in the SU(2) theory conducted by the Saclay group indicates that even a 32×16^3 lattice may not warrant $ma = 0.01$ [56][5].

According to the discussion in Chapter 4, we were decreasing quark mass successively, starting from the largest value of 0.16. For every ma we did enough iterations to reach

[5] The quenched QCD on a lattice up to 48×24^3 and at the quark masses down to 0.005, is being studied now by the Los Alamos group [57].

the accuracy $\Delta \sim 10^{-6}$ (cf. (4.8)) which was sufficient for the present purposes. This required 64 iterations for $ma = 0.016$ changed gradually to 200 at $ma = 0.0225$.

We would like to emphasize that all the results presented here are considered 1) as an illustration of the applicability of the ADI method, and 2) as an independent test of the conclusions of other authors obtained with different techniques. Our data are necessarily biased by the finite size effects and by large uncertainties in the extrapolation from $ma \geqslant 0.0225$. However, before we move to larger lattices (and hence larger computers), we felt it is necessary to check an overall performance of the new method on a smaller example.

A. Chiral properties of the theory

There are two ways of realizing continuous symmetries in Nature. In the Wigner mode, the physical states form irreducible representations of the symmetry group. On the other hand, the Goldstone-Nambu mode occurs when the ground state breaks spontaneously the symmetry of the interactions. Wigner multiplets do not occur in this case. Instead, massless Goldstone bosons appear for every broken direction in the group space. The latter scenario has been suspected for a long time to occur in strong interactions [58, 59, 60]. It was suggested by the lack of the degenerate in mass multiplets with opposite parity, and by the existence of the unusually light octet of pseudoscalar mesons. The symmetry in question is the $SU(3)_{left} \times SU(3)_{right}$ chiral symmetry of the flavour transformations. It is expected to be broken down to the diagonal $SU(3)_{vector}$ which shows up in the Wigner mode. Broken axial generators call for the massless pseudoscalar Goldstone bosons. The order parameter, which signals spontaneous breaking, is the quark condensate $\langle \bar{\psi}\psi \rangle$.

As was discussed in Chapter 2, Kogut-Susskind formulation of lattice fermions has enough remainders of the chiral symmetry to make the study of its spontaneous breaking feasible. Two generators of the remnant $U(1) \times U(1)$ symmetry are [32]

$$V = \mathbf{1} \otimes \mathbf{1} \quad \text{and} \quad A = \gamma_5 \otimes t_5, \tag{5.1}$$

where V corresponds to the continuum $U(1)_V$, and A generates the only part of the $SU(4)_A$ which remains on a lattice. It is *not* the continuum $U(1)_A$, since A has a nontrivial flavour structure. It was shown in the strong coupling limit that $\langle \bar{\psi}\psi \rangle \sim \langle \bar{\chi}\chi \rangle$ is non zero for $ma \to 0$, and hence that the strong coupling vacuum breaks the invariance generated by A. A mass of the flavour non-singlet pseudoscalar state was also shown to vanish in the chiral limit [32].

Nonperturbative study in the continuum limit can be done only with the aid of lattice Monte Carlo and is the subject of rather vigorous activity [61–66]. We begin with the quark condensate. For two light flavours, $\langle \bar{\psi}\psi \rangle$ is given by

$$a^3 \langle \bar{\psi}\psi \rangle = \tfrac{1}{2} \langle \bar{\chi}\chi \rangle = \tfrac{1}{2} \sum_{a=1}^{3} \langle G_{aa}(0, 0, [U]) \rangle_U, \tag{5.2}$$

where the propagator of a χ field is obtained from (2.7) and (3.9)

$$G_{ab}(m, n) = (M_\chi^{-1}[U])^{ab}_{mn}. \tag{5.3}$$

Our results for $\langle\bar{\psi}\psi\rangle$ are shown in Fig. 5 together with the quadratic extrapolation towards $ma = 0$. We obtain for the intercept,

$$a^3\langle\bar{\psi}\psi\rangle|_{ma=0} = 0.05(1), \tag{5.4}$$

indicating spontaneous breaking of the chiral symmetry. This number and our results for finite quark masses agree with those quoted by other authors [62–64]. Of course, the extrapolation to $ma = 0$ introduces a systematic error which can be only crudely estimated. We did that by removing the last data point from the fit and comparing the resulting intercepts. The difference was the same as the uncertainty caused by the propagation of the statistical errors quoted in (5.4).

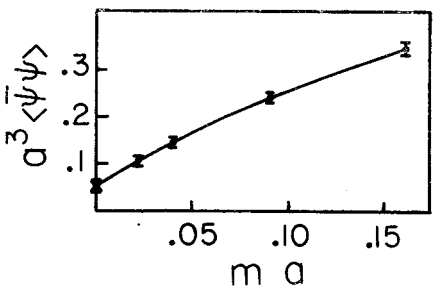

Fig. 5. The quark condensate, as measured for $ma = 0.016$, 0.09, 0.04 and 0.0225. The line shows the quadratic fit and the extrapolation to $ma = 0.0$

We move now to the Goldstone boson sector. Integrated pseudoscalar propagator (3.21) receives contributions only from the pion and its recurrences. Our results are shown in Fig. 6 for a range of quark masses. Indeed, no oscillatory component, characteristic of the $(-1)^{n_t}$ factors in Eqs (3.30), is seen. This demonstrates that there is no 0^{+-} partner of a pion, in accord with the nonrelativistic quark model. Any exotic state, which could contribute to this channel from pure symmetry considerations, is ruled out. This agrees with earlier results [62–65].

We have fitted $M_{PS}(n_t)$ with the formula (3.30) including one excited state in a pion channel. All 16 points in n_t were used. We did not symmetrize with respect to $n_t = T/2$. Fits were repeated removing one, two or three points closest to the source, in order to check stability of resulting parameters. As usual, if one removes too many small n_t points, the fit becomes unconstraint. Keeping small n_t data points does not meet the large n_t requirement and results in higher χ^2. One looks then for the intermediate value of the cut-off $n_t^{\min}$ which fulfills all three requirements: good fit, small errors, and reasonable stability. Fits were done with the aid of the CERN MINUIT program and errors on masses correspond to the change of χ^2 by 1.

Statistical errors grow larger with decreasing mass of a quark. For heavy quarks, effect of the gauge field is small compared to the rest energy of the constituents. In the chiral limit, interaction energy dominates and propagators are more sensitive to the fluctuations of the link variables. Consequently, all fits become more difficult for smaller ma.

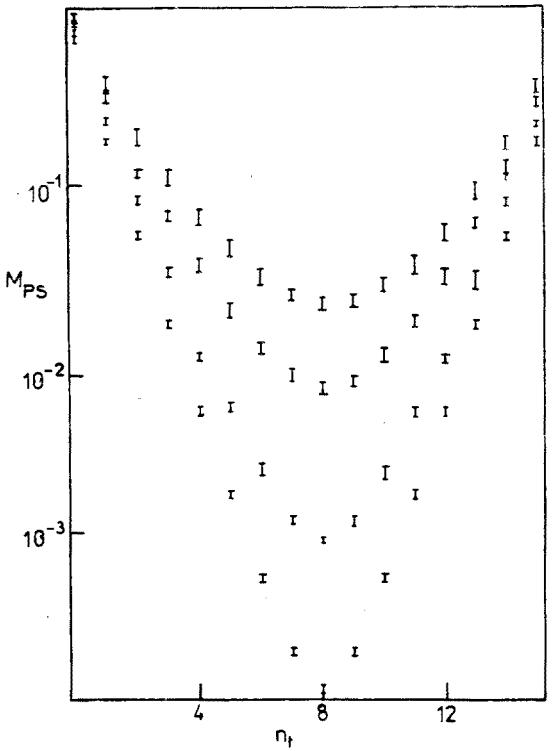

Fig. 6. The pseudoscalar propagator $M_{PS}(n_t)$ measured for four values of the quark mass ma

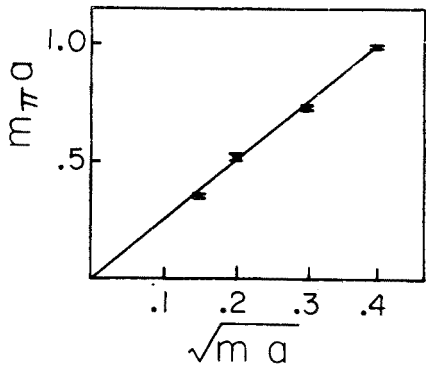

Fig. 7. The mass of a pseudoscalar state versus $\sqrt{ma}$. The linear fit is described in the text

For the pseudoscalar propagator, a signal to noise ratio is high since there are no cancellations in the MC prescription for M_{PS} (cf. Eqs (3.21) and (3.29)). Our two state (four parameters) fits were stable for $n_t^{min} = 0, 1, 2, 3$ and for all quark masses. Pion mass is shown in Fig. 7 together with the fit linear in $\sqrt{ma}$. The fit nicely extrapolates to zero as it should for the Goldstone boson. The linear dependence on $\sqrt{ma}$ is expected from the

current algebra. The Gell-Mann-Oakes-Renner relation reads:

$$m_\pi^2 f_\pi^2 = m\langle\bar{\psi}\psi\rangle, \tag{5.5}$$

and together with the data from Fig. 7 gives

$$\omega = \sqrt{2a\langle\bar{\psi}\psi\rangle}/f_\pi = 2.46(5). \tag{5.6}$$

This number agrees with the data of Barkai et al. and of other authors [63, 65]. Eqs (5.4) and (5.6) will be used shortly to determine the pion coupling constant f_π.

The signal for π' is also clear, the mass is stable, within larger errors, for $n_t^{\min} < 3$. The one-state fit to M_{PS} gives worse χ^2 and overestimates the pion mass. Only with a π' included is the behaviour of m_π consistent with the relation (5.5).

Vanishing of a pion mass in the chiral limit is a consequence of the Goldstone theorem applied to the relict U(1) symmetry of K–S fermions. Once a non-zero value of $\langle\bar{\psi}\psi\rangle$ has been measured, a massless state in the $\gamma_5 \otimes t_5$ channel has to occur. Less obvious is the problem of restoration and subsequent spontaneous breakdown of the remaining part of the $SU(4)_A$ group. This requires study of the more general currents (3.27) which lead to the nonlocal operators in the χ representation and will not be studied here. For the SU(2) case, this question was addressed by Billoire et al. [37] who presented a numerical evidence for the onset of the degeneracy of non-local would-be Goldstone bosons with the one in the $\gamma_5 \otimes t_5$ channel. Similar study for the SU(3) gauge group is being conducted by the Los Alamos group [57].

Coming back to the Gell-Mann-Oakes-Renner relation, we note that it is expected to work only for small ma. On the other hand, Fig. 7 and similar results of others, show that it is valid in much wider range of quark mass. From these two facts we conclude that f_π^2 must have the same dependence on ma as $\langle\bar{\psi}\psi\rangle$. Otherwise, the graph in Fig. 7 would not be linear. Indeed, very precise recent measurements of the Saclay group [56] show that the pion mass is not proportional to $\sqrt{ma}$ for very small quark mass $ma \sim 0.01$. This indicates that f_π^2 and $\langle\bar{\psi}\psi\rangle$ may differ at small ma. For larger ma, however, the linear regime remains [50].

B. A rho mass and the lattice scale

Vector-tensor propagator was measured according to the expression (3.26a). It is more sensitive to statistical fluctuations due to the cancellations implied by this formula. Physically, correlation length ($\xi_{VT} \sim 1/m_\varrho a$) in this channel is smaller, and thus the propagator falls more rapidly in n_t what results in bigger relative errors. Our data show clearly the oscillatory behaviour indicating that both parity partners couple to this channel. Two-state fit (3.30b) was stable but within larger than for M_{PS} errors, and only for $n_t^{\min} = 2.3$. The rho mass and its linear extrapolation are shown in Fig. 8 together with masses of other states.

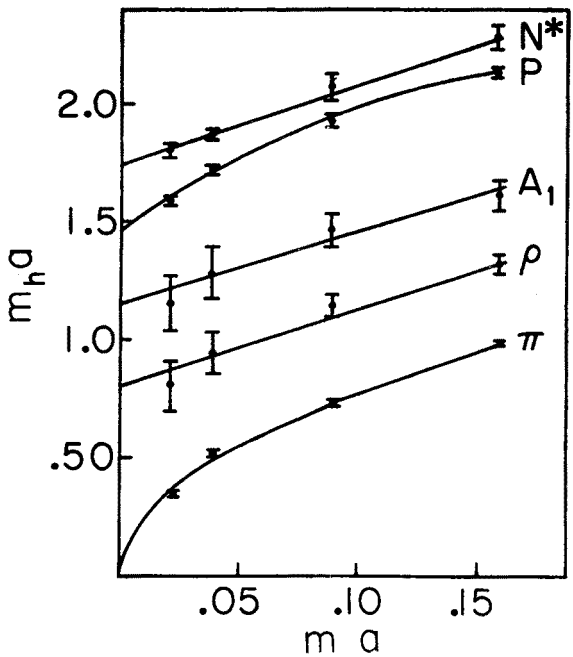

Fig. 8. Masses of the lowest lying hadrons. Lines represent the linear or quadratic fits to the *ma* dependence

Physical values of the pion and rho masses were used to fix the quark mass and the lattice constant a. We obtain

$$m = (m_u + m_d)/2 = 3.4 \text{ MeV}, \tag{5.7a}$$

$$a^{-1} = 0.93 \text{ GeV}. \tag{5.7b}$$

The main uncertainty of these estimates comes from poor determination of the rho mass and, consequently, from the freedom of the extrapolation. Change of m_ϱ within one standard deviation gives:

$$3.1 \text{ MeV} < m < 4.2 \text{ MeV}, \tag{5.8a}$$

$$0.91 \text{ GeV} < a^{-1} < 1.05 \text{ GeV}. \tag{5.8b}$$

Our numbers (5.7) are consistent with the results of Gilchrist et al. [64] and Bowler et al. [65] obtained on the lattice of the same size. However, our a^{-1} is smaller than the one obtained by Barkai et al. [62]. Technically, the difference comes from our higher value of the rho mass measured in lattice units. This is what one would expect from finite size effects[6].

[6] No agreement has been reached yet on the precise value of the lattice scale a. Various authors quote a^{-1} in the range (0.9–2.1) GeV [62–66]. Larger lattices favour $1.5 < a^{-1} < 2.0$.

Having fixed lattice scale, we can determine now other quantities in physical units. Renormalization group invariant value of the quark condensate is given by [67, 64]:

$$\langle\bar{\psi}\psi\rangle_{\text{inv}} = \alpha^{4/11}\langle\bar{\psi}\psi\rangle, \quad \alpha = \frac{3}{2\pi(\beta-2.74)}. \tag{5.9}$$

Our result (5.4) gives for the contribution from one flavour

$$\langle\bar{u}u\rangle = 0.5\langle\bar{\psi}\psi\rangle_{\text{inv}} = [215(15)\ \text{MeV}]^3, \tag{5.10}$$

what compares nicely wih the experimental value 225 ± 25 MeV [68][7].

From the slope (5.6) and from $a^3\langle\bar{\psi}\psi\rangle$ we obtain for the pion coupling constant

$$f_\pi = 120(10)\ \text{MeV} \quad (\text{exp: } 130\ \text{MeV}), \tag{5.11}$$

what again compares favourably with experiment. Our errors do not include uncertainty in the determination of a^{-1} which would add 10% to the relative error of all presented here results.

C. Other masses

Figure 8 summarizes our results on the spectrum of low-lying hadrons. Propagators were measured and analysed according to the Eqs (3.26b, c, 3.37) and (3.30c, d, 3.38). Quality of fits was similar to the vector case. Good χ^2 was achieved, although fits were stable only within large errors and in the limited range of $n_t^{\min}$ and ma. The scalar and pseudovector amplitudes also show oscillatory component as expected from Eqs (3.30). Hence, the $\tilde{\pi}$ and $\tilde{\varrho}$ states contribute to M_S and M_{PV}. Their masses are consistent with the ones extracted from the pseudoscalar and vector channels. This is encouraging and agrees with the observations of other authors but it is too early to draw definite conclusions about the restoration of the SU(4) symmetry.

In the three-quark channel, we have measured only the correlation between the local operators (3.32a) which is dominated by a proton and an N(1/2$^-$) resonance (3.38). In addition to the oscillatory component, baryonic propagator shows a regular change of sign, coming from the contribution of the antiparticles. This was clearly seen.

Baryonic correlation seems to be less fluctuating with the gauge configurations. This may indicate that we are still in the static quark regime, where the large mass of three constituents governs mainly the time decay of the correlation function. The same conclusion is also indicated by the large ratio of the proton to rho masses (see Fig. 9) which is the common disease of simulations with heavy quarks [41, 51, 63, 66]. For larger lattices ($ma = 0.01$) this number goes down to 1.4 [62] and the remaining discrepancy (experimentally $m_p/m_\varrho = 1.2$) can be blamed on the quenched approximation. Our number is consistent with the result of the Edinburgh group obtained on a lattice of the same size [51].

[7] We were unable to get this number from the raw data and the scale a quoted in Ref. [62].

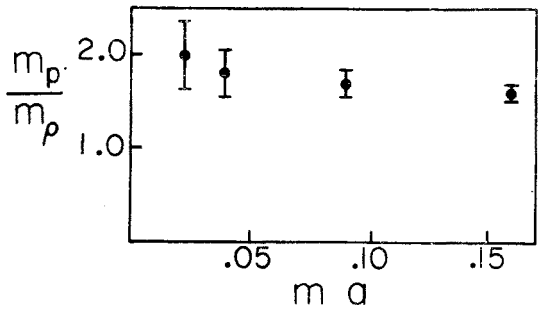

Fig. 9. The ratio of a proton to rho masses measured for $ma = 0.016$, 0.09, 0.04 and 0.0225

With the lattice scale determined in (5.7), the physical masses of non-strange hadrons read:

$$m_{A_1} = 1070\,(100)\ \text{MeV} \qquad (1270\ \text{MeV}),$$

$$m_B = 930\,(100)\ \text{MeV} \qquad (1230\ \text{MeV}),$$

$$m_S = 740\,(60)\ \text{MeV} \qquad (980\ \text{MeV}),$$

$$m_p = 1360\,(60)\ \text{MeV} \qquad (940\ \text{MeV})$$

and 10% of the relative uncertainty in a^{-1} should be added to the above errors. Clearly, there is a room for improvement. We would like to emphasize, however, that the main difficulty in extracting physical masses in the chiral limit is caused by rather weakly constrained extrapolation procedure towards $ma = 0$. Our "raw" data obtained at finite ma are consistent with those of other authors what shows that our method of computing quark propagators has passed the first test. Improving the quality of the extrapolation clearly depends on the available computing resources and is left for the future.

We move now to strange particles. Using kaon mass as an input, we obtain from the pseudoscalar propagator

$$m_s = 90\ \text{MeV}.$$

Then, the masses of K* and φ are predicted to be:

$$m_{K^*} = 890\ \text{MeV} \qquad (892\ \text{MeV}),$$

$$m_\varphi = 1050\ \text{MeV} \qquad (1070\ \text{MeV}).$$

This agreement with the experiment is not surprising, since the vector propagator was earlier used to fix a lattice constant. Therefore, we conclude only that the dependence of the vector meson mass on the quark mass is correctly reproduced by lattice simulation.

D. f_K/f_π

Recently, Billoire et al. determined the ratio $\xi = f_K/f_\pi$ using additional information contained in the residue R of the pseudoscalar propagator [56]. They did it for a SU(2) theory. Our data allow us to repeat their analysis for the SU(3) case.

From the sum rule

$$G_{aa}(0,0) = ma \sum_{n,b} |G_{ab}(0,n)|^2 \tag{5.12}$$

and from the Gell-Mann-Oakes-Renner relation (5.5), one obtains

$$(af_P)^2 = \frac{2(ma)^2}{(m_P a)^3} R_P(ma), \tag{5.13}$$

where P denotes a pseudoscalar at the quark mass ma, and R_P is the residue of the pseudoscalar propagator at the bound state mass $m_P a$. According to the definition of the coupling constant f_P, contributions from the higher excitations have been dropped from the RHS of (5.13). From (5.13), one can directly determine dependence of f_P on the quark mass. Our data on $R_P(ma)$ and $m_P a(ma)$ lead to the following linear parametrization:

$$f_P^2 a^2 = A + Bma = 0.0024\,(6) + 0.084\,(5)\, ma. \tag{5.14}$$

It is clear from (5.14) that $f_\pi = f_P(0)$ is poorly determined by the data. Therefore it is not advisable to use (5.13) directly to calculate the ratio ξ. Instead, one uses the relation

$$m_P^2 a^2 = \omega^2 ma, \quad \omega = 2.46\,(5), \tag{5.15}$$

which we have found to work nicely over a large range of the quark mass (cf. Fig. 7 and Eq. (5.6.)). Eliminating ma one obtains for the ratio

$$\xi^2 = \frac{A + B\dfrac{m_K^2 a^2}{\omega^2}}{A + B\dfrac{m_\pi^2 a^2}{\omega^2}} = \frac{1 + \dfrac{B}{\omega^2}\dfrac{m_K^2}{f_\pi^2}}{1 + \dfrac{B}{\omega^2}\dfrac{m_\pi^2}{f_\pi^2}}. \tag{5.16}$$

In the last equality we have eliminated the troublesome parameter A by the physical value of the $f_\pi = f_P(0) = Aa^{-2}$. Inserting our results for the slopes B and ω^2 gives

$$\xi = 1.16(2)$$

to be compared with the experimental value 1.22(1) [68]. Billoire et al. obtain 1.24(6) from their SU(2) data at $\beta = 2.5$. This nice result was achieved by trading two poorly defined parameters A and a for the physical value of f_π and the better measured slope ω.

6. Summary and conclusions

Propagator of a quark in arbitrary external field is the basic ingredient in the Monte Carlo simulations of lattice gauge theories with fermions. In quenched and unquenched formulations a quark propagator is the building block of all fermionic observables. It is also required during the generation of the gauge field configurations sensitive to dynamical fermions.

We have computed the spectrum of the lowest lying hadrons in quenched quantum chromodynamics applying a novel technique to obtain quark propagators. The Kogut-Susskind formulation of lattice fermions was used. We have also presented the straightforward construction of various channels in the naive formulation. It is much simpler and gives the same results as staggered approach. It also shows clearly the interplay between additional modes in producing the final composition of various channels.

Our algorithm is based on the Alternate Direction Implicit method of inversion of the large sparse matrices. It has a property of dimensional reduction — four-dimensional propagation of a quark is built from a series of, partly decoupled, propagations in two-dimensional worlds. Apart from the physical appeal and (unexplored yet) possibility of analytical approach, this technique is well suited for parallel processing used commonly for solving problems of this size. The method is converging for small mass of a quark ($ma = 0.01$) and is found to be a useful alternative to the generally applied conjugate gradient algorithm.

The aim of this work is twofold. We wanted to test a new approach in the realistic circumstances which would expose our algorithm to all difficulties of the "real world", i.e. small ma, large-size problem, and fluctuating quantum background field. Secondly, our data can serve as an independent test of the results obtained by other authors.

Altogether results discussed in the previous chapter are rather satisfactory. Chiral properties of the theory come out consistently and agree with the findings of other authors. Statistical errors in the Goldstone boson channel are reasonably small, eliminating at least one uncertainty in the extrapolation towards the chiral limit. The problem of systematic errors introduced by the extrapolation is, of course, open. Its ultimate solution can be achieved only by performing lattice Monte Carlo *at* the physical value of the quark mass, which is still three times smaller than ma attainable in recent simulations. From our data, we estimate $ma_{\text{phys}} = 0.0037(6)$. Apart from this difficulty, which is common to all lattice computations, our raw data are consistent with those of other authors at overlapping values of quark mass. Dependence on the ma in the range between non-strange and strange quarks is also correct. The latter observation applies not only to the slope, but also to the residue of the pseudoscalar propagator as confirmed by the reasonable result for f_K/f_π. To our knowledge, this number was extracted earlier only from the SU(2) data.

Other mesonic propagators have larger statistical errors, and hence the analysis of these channels provides only qualitative information. Nevertheless, the general pattern of various parity mixings is clearly seen and supplies additional tests of the present approach. Similar conclusion follows also from the study of the baryonic channel. Peculiar to staggered fermions, structure of the propagator is evident in the data. Ratio of the proton and rho masses is consistent with data of other groups, and higher than the experimental value.

One must remember, however, that any comparison with the experiment is subject to the limitations of the quenched approximation. For this reason, we have concentrated rather on the consistency with other authors. To conclude, we think that the ADI technique has passed its first nontrivial trial and can be readily applied to yet larger scale computations of the hadronic properties.

I would like to thank Doc. R. Wit for bringing the ADI methods to my attention. Calculations described in this paper were done in Wuppertal during the fellowship of the Alexander von Humboldt Foundation. I would like to thank the Theory Group in Wuppertal for their hospitality and for the stimulating interest. I also thank Professor H. Zoller for his kind assistance while I was using the CYBER 205 computer in the Computing Center of the Ruhr-University in Bochum. I would like to thank Dr. J. Karczmarczuk for the critical reading of the manuscript.

APPENDIX

We shall derive here the quantum number content of the vector-tensor, pseudo-vector and the scalar propagators which were defined in Eqs (3.26).

Consider, for simplicity, the contribution from one polarisation ($i = 1, 2, 3$) to the vector propagator (3.26a)

$$M^i_{\mathrm{VT}}(n_t) = \sum_{\vec{n}} (-1)^{n_t} K(n) = \sum_{\vec{n}} (-1)^{n\cdot\eta^{(i)}} \operatorname{Tr}\{\gamma^5 S(n)\gamma^5 S(-n)\} \tag{A1}$$

with $\eta^{(i)}_\mu = 0$ for $\mu \neq i$ and $\eta^{(i)}_i = 1$. Using (3.18) we obtain

$$M^i_{\mathrm{VT}} = \sum_{\vec{n}} \sum_{\eta\eta'} (-1)^{n\cdot(\eta-\eta'+\eta^{(i)})} \operatorname{Tr}\{\gamma^5 S_{\mathrm{F}}(x_\eta)\gamma^5 S_{\mathrm{F}}(-x_{\eta'})\}. \tag{A2}$$

$$M^i_{\mathrm{VT}} \equiv A^i_{\mathrm{VT}}(n_t) + (-1)^{n_t} B^i_{\mathrm{VT}}(n_t).$$

Only terms without the oscillating factors survive in the continuum limit, hence $\eta' = \eta + \eta^{(i)}$ for the A^1_{VT}, and $\eta' = \eta + \eta^{(i)} + \eta^{(4)} \equiv \eta + \eta^{(4i)}$ for the B^1_{VT} amplitude, where $\eta^{(4)}_4 = 1$, $\eta^{(4)}_j = 0$. Consequently,

$$A^i_{\mathrm{VT}} = \sum_{\vec{n}} \sum_{\eta} \operatorname{Tr}\{\gamma^5 S_{\mathrm{F}}(x_\eta)\gamma^5 S_{\mathrm{F}}(-x_{\eta+\eta^{(i)}})\}. \tag{A3}$$

This can be further simplified with the aid of Eq. (3.23)

$$\begin{aligned} A^i_{\mathrm{VT}} &= \sum_{\vec{n}} \sum_{\eta} \operatorname{Tr}\{\Gamma_\eta S_{\mathrm{F}}(x)\Gamma^\dagger_\eta \Gamma_{\eta+\eta^{(i)}} S_{\mathrm{F}}(-x)\Gamma^\dagger_{\eta+\eta^{(i)}}\} \\ &= 16 \sum_{\vec{n}} \operatorname{Tr}\{\Gamma^\dagger_{\eta^{(i)}} S_{\mathrm{F}}(x)\Gamma_{\eta^{(i)}} S_{\mathrm{F}}(-x)\}, \end{aligned} \tag{A4}$$

where we have used the following property of Γ_η (cf. the definition (3.13)):

$$\Gamma_\eta \Gamma_{\eta+\xi} = \varepsilon(\eta, \xi)\Gamma_\xi, \qquad \varepsilon^2(\eta, \xi) = 1. \tag{A5}$$

For the B amplitude one obtains:

$$B^i_{\mathrm{VT}} = \sum_{\vec{n}} \sum_{\eta} \operatorname{Tr}\{\gamma^5 S_{\mathrm{F}}(x_\eta)\gamma^5 S_{\mathrm{F}}(-x_{\eta+\eta^{(4i)}})\}$$

$$= \sum_{\vec{n}} \sum_{\eta} \mathrm{Tr}\,\{\gamma^5 \Gamma_\eta S_F(x) \Gamma_\eta^\dagger \gamma^5 \Gamma_{\eta+\eta^{(4i)}} S_F(-x) \Gamma_{\eta+\eta^{(4i)}}^\dagger\}$$

$$= 16 \sum_{\vec{n}} \mathrm{Tr}\,\{\gamma^5 \Gamma_{\eta^{(4i)}}^\dagger S_F(x) \gamma^5 \Gamma_{\eta^{(4i)}} S_F(-x)\}. \tag{A6}$$

Note, that the γ^5 matrix appears in the final answers (A4) and (A6) only for even $\eta - \eta'$.

Similar considerations give for the pseudovector amplitudes

$$A_{PV}^{ik} = 16 \sum_{\vec{n}} \mathrm{Tr}\,\{\Gamma_{\eta^{(ik)}}^\dagger \gamma^5 S_F(x) \gamma^5 \Gamma_{\eta^{(ik)}} S_F(-x)\}, \tag{A7}$$

$$B_{PV}^{ik} = 16 \sum_{\vec{n}} \mathrm{Tr}\,\{\Gamma_{\eta^{(4ik)}}^\dagger S_F(x) \Gamma_{\eta^{(4ik)}} S_F(-x)\}, \tag{A8}$$

and for the scalar propagators

$$A_S = 16 \sum_{\vec{n}} \mathrm{Tr}\,\{\Gamma_{\eta^{(123)}}^\dagger S_F(x) \Gamma_{\eta^{(123)}} S_F(-x)\}, \tag{A9}$$

$$B_S = 16 \sum_{\vec{n}} \mathrm{Tr}\,\{S_F(x) S_F(-x)\}, \tag{A10}$$

where

$$\eta_\mu^{(ik)} = 0, \quad \mu \neq i, k; \quad \eta_\mu^{(ik)} = 1, \quad \mu = i, k; \quad \eta^{(4ik)} = \eta^{(ik)} + \eta^{(4)};$$

$$\eta^{(1,2,3)} = (1, 1, 1, 0).$$

Formulas (A4) and (A6)–(A10) justify the assignment of various operators listed in Table I.

REFERENCES

[1] K. G. Wilson, *Phys. Rev.* **D10**, 2445 (1974).

[2] For a recent review see: A. Hasenfratz, P. Hasenfratz, *Ann. Rev. Nucl. Part. Sci.* **35**, 559 (1985); see also in *Advances in Lattice Gauge Theory*, eds D. W. Duke, J. F. Owens, World Scientific 1985.

[3] B. Barkai, D. Moriarty, C. Rebbi, *Phys. Rev.* **D30**, 1293 (1984); P. de Forcrand, unpublished (1985); K. C. Bowler et al., Amsterdam preprint ITFA-85-07, 1985.

[4] B. Berg, A. Billoire, *Nucl. Phys.* **B226**, 405 (1983); P. de Forcrand et al., preprint DESY/LAPP-TH-119, 1984; *Phys. Lett.* **152B**, 107 (1985).

[5] T. Čelik, J. Engels, H. Satz, *Phys. Lett.* **125B**, 411 (1983); J. B. Kogut et al., *Phys. Rev. Lett.* **150**, 393 (1983); A. Kennedy et al., *Phys. Lett.* **155B**, 414 (1985); for recent review see: H. Satz, *Ann. Rev. Nucl. Part. Sci.* **35**, 245 (1985).

[6] K. G. Wilson, J. B. Kogut, *Phys. Rep.* **12C**, 75 (1974); R. H. Swendsen, *Phys. Rev. Lett.* **42**, 859 (1979).

[7] K. Bowler et al., *Nucl. Phys.* **B257**, 155 (1985).

[8] F. A. Berezin, *The Method of Second Quantization*, Academic Press, New York 1966.

[9] J. B. Kogut, in *Advances in Lattice Gauge Theory*, eds D. W. Duke, J. F. Owens, World Scientific 1985.

[10] C. Rebbi, talk presented at the Wuppertal meeting on large scale simulations of Lattice Gauge Theories, Wuppertal 1985.

[11] I. Schmidt, talk given at the Wuppertal meeting, 1985.

[12] F. Fucito, S. Solomon, *Phys. Rev. Lett.* **55**, 2641 (1985).
[13] F. Fucito, E. Marinari, G. Parisi, C. Rebbi, *Nucl. Phys.* **B180** [FS2], 369 (1981); D. Weingarten, D. Petcher, *Phys. Lett.* **99B**, 333 (1981).
[14] D. Callaway, A. Rahman, *Phys. Rev. Lett.* **49**, 613 (1982); J. Polonyi, H. W. Wyld, *Phys. Rev. Lett.* **51**, 2257 (1983); J. Polonyi et al., *Phys. Rev. Lett.* **53**, 644 (1984).
[15] J. Klauder, Lecture at the XXII Internationale Universitätswochen für Kernphysik, Schladming 1983.
[16] H. Gausterer, J. Klauder, preprint UNIGRAZ-UTP 11/85.
[17] J. Wosiek, *Acta Phys. Pol.* **B13**, 543 (1982).
[18] D. Weingarten, *Phys. Lett.* **109B**, 57 (1982).
[19] H. Hamber, G. Parisi, *Phys. Rev. Lett.* **47**, 1792 (1981); E. Marinari, G. Parisi, C. Rebbi, *Phys. Rev. Lett.* **47**, 1795 (1981).
[20] D. Weingarten, *Nucl. Phys.* **B257** [FS14], 629 (1985).
[21] G. G. Batrouni et al., *Phys. Rev.* **D32**, 2736 (1985).
[22] M. Creutz, *Phys. Rev.* **D15**, 1128 (1977); M. Luscher, *Comm. Math. Phys.* **54**, 283 (1977); H. S. Sharatchandra, H. J. Thun, P. Weisz, *Nucl. Phys.* **B192**, 205 (1981).
[23] R. P. Feynman, A. R. Hibbs, *Quantum Mechanics and Path Integrals*, Mc Graw-Hill, New York 1965.
[24] H. B. Nielsen, M. Ninomya, *Nucl. Phys.* **B185**, 20 (1981); **B193**, 173 (1981).
[25] J. B. Kogut, in *Recent Advances in Field Theory and Statistical Mechanics*, eds J. B. Zuber, R. Stora, Les Houches, 1982.
[26] J. Smit, *Acta Phys. Pol.* **B17**, 531 (1986).
[27] D. Weingarten, Preprint, IUHET-82, 1982.
[28] G. G. Batrouni, in *Advances in Lattice Gauge Theory*, eds D. Duke, J. F. Owens, World Scientific 1985.
[29] A. König, K. H. Mütter, K. Schilling, J. Smit, Wuppertal preprint, WU B 85-11, 1985.
[30] G. W. Kilcup, talk given at the Wuppertal meeting, Wuppertal, November 1985.
[31] J. B. Kogut, L. Susskind, *Phys. Rev.* **D9**, 3501 (1974); L. Susskind, *Phys. Rev.* **D16**, 3031 (1977).
[32] H. Kluberg-Stern, A. Morel, O. Napoly, B. Petersson, *Nucl. Phys.* **B220** [FS8], 447 [1983].
[33] M. F. L. Golterman, J. Smit, *Nucl. Phys.* **B245**, 61 (1984).
[34] C. van den Doel, J. Smit, *Nucl. Phys.* **B228**, 122 (1983).
[35] N. Kawamoto, J. Smit, *Nucl. Phys.* **B192**, 100 (1981).
[36] M. F. L. Golterman, J. Smit, *Nucl. Phys.* **B255**, 328 (1985).
[37] A. Billoire, R. Lacaze, E. Marinari, A. Morel, *Nucl. Phys.* **B251** [FS13], 581 (1985).
[38] M. F. L. Golterman, Amsterdam preprints, ITFA-85-05, March 1985; ITFA-86-4, February 1986.
[39] G. Kilcup, S. R. Sharpe, Harvard preprint.
[40] A. Morel, J. P. Rodriguez, *Nucl. Phys.* **B247**, 44 (1984).
[41] B. A. Berg, Tallahassee preprint, SCRI-FSU-85-8, Nov. 85.
[42] K. C. Bowler et al., *Phys. Lett.* **145B**, 88 (1984); I. M. Barbour et al., DESY preprint 84-087, LAPP-TH 118, 1984.
[43] M. R. Hestens, E. L. Steifel, *Nat. Bur. Std. J. Res.* **49**, 409 (1952); J. Stoer, R. Bulirsch, *Introduction to Numerical Analysis*, Springer-Verlag, Berlin 1980.
[44] E. L. Wachspress, *Iterative Solutions of Elliptic Systems*, Prentice-Hall 1966.
[45] J. Wosiek, *Phys. Lett.* in press.
[46] J. Wosiek, talk at the Wuppertal meeting, November 1985.
[47] A. Billoire, E. Marinari, G. Parisi, preprint 1985.
[48] J. Schwinger, *Phys. Rev.* **128**, 2425 (1962).
[49] K. D. Rothe, Heidelberg preprint, HD-THEP-85-21.
[50] J. Jolicoeur, A. Morel, *Nucl. Phys.* **B262**, 627 (1985).
[51] D. J. Wallace, private communication.
[52] B. Bunk, R. Sommer, Wuppertal preprint, WU-B-85-8, 1985.

[53] A. König, K. H. Mütter, K. Schilling, *Phys. Lett.* **147B**, 145 (1984).
[54] K. H. Mütter, K. Schilling, *Nucl. Phys.* **B230** [FS10], 275 (1984).
[55] D. Barkai, K. J. M. Moriarty, C. Rebbi, CERN preprint, CERN-TH.4065/84.
[56] A. Billoire et al., Saclay preprint, Saclay PhT 85-180, November 1985.
[57] S. R. Sharpe, Harvard preprint, HUTP-85/A077, 11/85.
[58] J. Goldstone, *Nuovo Cimento* **19**, 154 (1961); Y. Nambu, G. Jona-Lasinio, *Phys. Rev.* **122**, 345 (1961).
[59] M. Peskin, in *Recent Advances in Field Theory and Statistical Mechanics*, ed. J. B. Zuber, R. Stora, Les Houches 1982.
[60] J. Goldstone, A. Salam, S. Weinberg, *Phys. Rev.* **127**, 965 (1962).
[61] I. M. Barbour et al., *Phys. Lett.* **158B**, 61 (1985); A. D. Kennedy et al., *Phys. Rev. Lett.* **54**, 87 (1985).
[62] D. Barkai, K. J. M. Moriarty, C. Rebbi, CERN, Feb. 85.
[63] A. Billoire, E. Marinari, R. Petronzio, *Nucl. Phys.* **B251** [FS13], 141 (1985).
[64] J. P. Gilchrist et al., *Nucl. Phys.* **B248**, 29 (1984).
[65] K. C. Bowler et al., *Nucl. Phys.* **B240** [FS12], 213 (1984).
[66] R. Gupta, A. Patel, *Nucl. Phys.* **B226**, 152 (1983).
[67] E. Marinari, G. Parisi, C. Rebbi, *Nucl. Phys.* **B190** [FS3], 734 (1981).
[68] J. Gasser, H. Leutwyller, *Phys. Rep.* **87C**, 78 (1982).